NON-DARCY NATURAL CONVECTION FROM ARBITRARILY INCLINED HEATED SURFACES IN SATURATED POROUS MEDIA

By D. S. RILEY *and* D. A. S. REES

(*School of Mathematics, University Walk, Bristol* BS8 1TW)

[Received 11 January 1984. Revise 29 May 1984]

SUMMARY

An analysis is presented of steady free convection in a saturated porous medium bounded by a heated flat surface and a second thermally insulated (or cold) flat surface, which forms a wedge of angle α. The flow is induced by the heated surface, which is at an angle δ to the gravity vector, where $-\frac{1}{2}\pi < \delta \leqslant \frac{1}{2}\pi$. The pressure-gradient–velocity relation is taken to be nonlinear, with departure from the linear Darcy situation measured by a parameter G. Matched asymptotic expansions are employed in analysing two distinct cases: the heated surface is (i) horizontal and (ii) at a finite angle above the horizontal. In the former case the flow is driven along by a buoyancy-induced pressure gradient, whilst in the latter it is the direct action of buoyancy forces that drives the flow. Extensive consideration is given to the effects of varying α, δ and G.

1. Introduction

CONVECTIVE flows in porous media are of interest in many varied situations, for example in geothermal energy resource and oil-reservoir modelling, in the analysis of insulating systems and in flows through tobacco rods. There is a plethora of literature covering these situations, most of which concentrates on the classical Darcy-flow case. It is known, however, that at higher flow rates or in highly porous media there is a departure from the linear law and inertial effects become important. In terms of the Reynolds number based on a typical particle diameter (say), it has been found that the flow becomes non-Darcian when the Reynolds number exceeds unity (**1**). Physically, this departure is believed to be due to flow separation within the medium, whilst mathematically it manifests itself as a nonlinear term in the velocity–pressure-gradient relationship. The particular problem that we wish to address in this paper is the non-Darcian buoyancy-induced boundary-layer flow due to a heated inclined flat surface bounding a wedge-shaped saturated isotropic porous medium.

The corresponding Darcian situations have been considered by Cheng and his co-workers (**2** to **5**), whilst a matched asymptotic analysis of the vertical configuration has recently been carried out by Daniels and Simpkins (**6**). There seems to be only one paper† in the literature dealing with the

† A further paper (**13**) appeared after this present paper had been submitted.

non-Darcian case: Plumb and Huenefeld (**7**) considered non-Darcy natural convection in a saturated isotropic medium. They employed equations which are not invariant under rotations and therefore not strictly relevant to *isotropic* media. Fortunately, however, their equations took on the correct form in the boundary-layer limit. It should be noted in passing that they quote a one-dimensional model equation of Forchheimer which is also inappropriate for isotropic media. Finally it was stated in (**3**, **4**) that there is no boundary-layer solution for a non-vertical isothermal surface (Darcy flow). This however was implicitly retracted, at least in the horizontal case, by the appearance of (**5**) wherein a boundary-layer solution was determined.

In section 2 we derive the equations governing buoyancy-induced flows over generally inclined surfaces and then in sections 3 and 4 we analyse boundary-layer flows over horizontal heated surfaces and those inclined at finite angles *above* the horizontal, respectively. In the former case the flow is driven by a buoyancy-induced pressure gradient, whilst in the latter it is driven by the direct action of buoyancy forces. There is, of course, a range of inclinations (very near to the horizontal, in fact) where a transition regime exists when both driving mechanisms are present. This transition zone has a structure akin to that found by Jones (**8**) for a Newtonian fluid: the flow is driven initially by the induced pressure gradient but asymptotically by the buoyancy forces. The analysis of this transition problem will be considered in another report (**9**).

The analyses of the problems, using matched asymptotic expansions, are terminated at the appearance of eigensolutions. In the case of the inclined surface, the eigensolution is related to the usual leading-edge shift (**10**), whilst the precise nature of the eigensolution in the horizontal case is not clear. In the non-Darcian situation considered here, we find that we must include logarithmic terms in our asymptotic expansions, essentially because of the existence of the eigensolutions. This is in contrast to the Darcian situation (see (**6**)), where logarithms must again be included but via a different mechanism. There they are generated by a breakdown of the outer expansion and are dependent on the angle between the hot and cold or insulated surfaces.

In section 5 we consider the heat transfer from the hot surface and, using our asymptotic results, derive local heat-transfer values. These, however, give no information concerning the total heat output from the hot surface. Thus we follow Heiber (**11**) in considering the total convective heat transfer at any cross-section of the boundary layer, thereby obtaining global heat-transfer results and a measure of the leading-edge heat transfer.

Finally in section 6 we discuss our results.

2. Governing equations

The configuration is as shown in Fig. 1. The surface $y'=0$, $x'>0$ is isothermal at temperature T_1 whilst the ambient temperature of the satu-

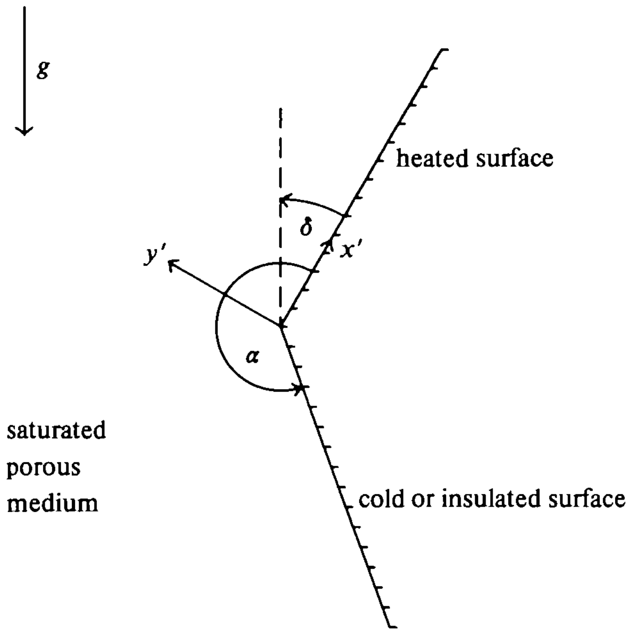

FIG. 1. Flow domain and coordinate system

rated medium is T_0. The other bounding surface is also at ambient temperature T_0 or is insulated—it has no effect on our analysis which condition we consider, as we neglect exponentially small terms (cf. (6)). We consider $T_1 > T_0$ and examine the resulting steady two-dimensional flow induced by buoyancy forces in the saturated porous medium. We take as our constitutive relation

$$-\frac{k}{\mu}[\operatorname{grad} p + \rho \mathbf{g}] = \left[1 + \frac{\tilde{k}}{\mu}\rho q\right]\mathbf{q},$$

where Darcy's law is recovered if $\tilde{k} = 0$. Here k is the permeability of the medium and $\tilde{k}$ is a material parameter which may be thought of as a measure of its inertial impedance; $\mathbf{q}$ is the velocity, ρ the fluid density, μ the coefficient of viscosity and p the total pressure. To illustrate how the additional nonlinear term comes into play when the porosity is high, we may quote Ergun's relations (see (7)) for k and $\tilde{k}$:

$$k = \frac{L^2\varepsilon^3}{150(1-\varepsilon)^2}, \qquad \tilde{k} = \frac{1{\cdot}75L}{150(1-\varepsilon)},$$

where ε denotes porosity and L the characteristic pore or particle diameter. Clearly when $\varepsilon \sim 1$, $\tilde{k}$ is large and the nonlinear term is important.

On assuming thermodynamic equilibrium between the porous matrix and the fluid and invoking the Boussinesq approximation, the governing equations become

$$\frac{\partial u}{\partial x'}+\frac{\partial v}{\partial y'}=0, \tag{1}$$

$$\frac{k}{\mu}\left[-\frac{\partial p}{\partial x'}+\beta g\rho(T-T_0)\cos\delta\right]=\left[1+\frac{\tilde{k}}{\mu}\rho q\right]u, \tag{2}$$

$$\frac{k}{\mu}\left[-\frac{\partial p}{\partial y'}+\beta g\rho(T-T_0)\sin\delta\right]=\left[1+\frac{\tilde{k}}{\mu}\rho q\right]v, \tag{3}$$

$$u\frac{\partial T}{\partial x'}+v\frac{\partial T}{\partial y'}=\kappa\left[\frac{\partial^2 T}{\partial x'^2}+\frac{\partial^2 T}{\partial y'^2}\right], \tag{4}$$

where $\mathbf{q}=(u, v)$, T is the temperature, β the coefficient of cubical expansion and κ the effective thermal diffusivity. Introducing non-dimensional variables

$$(x', y')=\frac{\mu\kappa}{g\beta(T_1-T_0)k\rho}(x, y), \qquad \theta=\frac{T-T_0}{T_1-T_0}, \tag{5}$$

and a dimensionless stream function ψ such that

$$(u, v)=\left(\frac{g\beta(T_1-T_0)k\rho}{\mu}\right)\left(\frac{\partial\psi}{\partial y}, -\frac{\partial\psi}{\partial x}\right),$$

we obtain, on eliminating the pressure,

$$(1+GQ)\nabla^2\psi+Q^{-1}G(\psi_x^2\psi_{xx}+2\psi_x\psi_y\psi_{xy}+\psi_y^2\psi_{yy})=\theta_y\cos\delta-\theta_x\sin\delta \tag{6}$$

and

$$\psi_y\theta_x-\psi_x\theta_y=\nabla^2\theta. \tag{7}$$

In the above, ∇^2 denotes the two-dimensional Laplacian, $Q\equiv(\psi_x^2+\psi_y^2)^{\frac{1}{2}}$ is the dimensionless speed and G is the parameter $(\rho/\mu)^2 k\tilde{k}g\beta(T_1-T_0)$, which measures the inertial effects and is thought of as a modified Grashof number in (7).

In terms of the usual polar coordinates (r, ϕ) defined by

$$x=r\cos\phi, \qquad y=r\sin\phi,$$

the boundary condition may be expressed as

$$\left.\begin{array}{llll}\psi=0, & \theta=1 \text{ on } \phi=0, & & \\ \psi=0, & \theta=0 \text{ or } \partial\theta/\partial\phi=0 & \text{on} & \phi=\alpha, \\ \theta\to 0, & \psi=o(r) \text{ as } r\to\infty, & & 0<\phi<\alpha.\end{array}\right\} \tag{8}$$

3. The asymptotic structure as $r \to \infty$ for the horizontal configuration ($\delta = \frac{1}{2}\pi$)

A simple order-of-magnitude analysis suggests the form of solution valid near the hot horizontal boundary. In view of the boundary condition at the wall, we take $\theta = O(1)$ as $x \to \infty$, whilst on assuming that the temperature adjusts rapidly to its ambient value, (7) implies that $\psi = O(x/y)$ as $x \to \infty$. Finally from (6) $y = O(x^{\frac{2}{3}})$, which is exactly the similarity form found by Cheng and Chang (**5**). Thus it is assumed that, in the boundary layer, as $x \to \infty$,

$$\psi = x^{\frac{1}{3}} f_0(\eta) + \ldots, \qquad \theta = g_0(\eta) + \ldots,$$

where

$$\eta = y/x^{\frac{2}{3}}. \tag{9}$$

The functions f_0 and g_0 satisfy

$$f_0'' - \tfrac{2}{3}\eta g_0' = 0, \qquad g_0'' + \tfrac{1}{3} f_0 g_0' = 0, \tag{10a}$$

subject to

$$f_0(0) = 0, \qquad g_0(0) = 1, \tag{10b}$$

whilst in order to recover the ambient conditions,

$$f_0' \to 0, \qquad g_0 \to 0, \qquad \text{as} \quad \eta \to \infty. \tag{10c}$$

The flow is Darcian to this lowest order as might be expected since, in this configuration, the induced velocities are weak and consequently the non-linear terms are unimportant. This problem was solved numerically by Cheng and Chang (**5**) who found that, as $\eta \to \infty$,

$$f_0 \to 2{\cdot}813$$

and g_0 decays exponentially. We, however, re-solved the problem and found values of f_0 and g_0 which are in slight disagreement with their values. For example, we found that $f_0(\infty) = 2{\cdot}816$. Thus the boundary-layer flow entrains fluid from an outer region where the temperature is of exponentially small order. The fact that there are neither logarithmic nor algebraic terms in the outer-temperature expansion can easily be proved mathematically as in (**6**), but we omit the details.

After further analysis, it becomes clear that in the boundary-layer region the solutions have the following expansions:

$$\left.\begin{aligned} \psi &= x^{\frac{1}{3}} f_0(\eta) + f_1(\eta) + x^{-\frac{1}{3}} \ln x\, \bar{f}_2(\eta) + x^{-\frac{1}{3}} f_2(\eta) + \ldots, \\ \theta &= g_0(\eta) + x^{-\frac{2}{3}} \ln x\, \bar{g}_2(\eta) + x^{-\frac{2}{3}} g_2(\eta) + \ldots, \end{aligned}\right\} \tag{11}$$

as $x \to \infty$. The terms of $O(x^{-\frac{1}{3}} \ln x)$ and $O(x^{-\frac{2}{3}} \ln x)$ have to be included in the ψ- and θ-expansions, respectively, in order to be able to solve the equations for f_2 and g_2.

In the outer region it proves convenient to use polar coordinates. On neglecting the temperature terms (which are exponentially small), the governing equation is

$$[1+G(\psi_r^2+r^{-2}\psi_\phi^2)^{\frac{1}{2}}](\psi_{rr}+r^{-1}\psi_r+r^{-2}\psi_{\phi\phi})+ \\ +\frac{G}{(\psi_r^2+r^{-2}\psi_\phi^2)^{\frac{1}{2}}}(\psi_r^2\psi_{rr}-r^{-3}\psi_r\psi_\phi^2+2r^{-2}\psi_r\psi_\phi\psi_{r\phi}+r^{-4}\psi_\phi^2\psi_{\phi\phi})=0, \quad (12)$$

and the formal expansion is

$$\psi=r^{\frac{1}{2}}F_0(\phi)+F_2(\phi)+\ldots \quad \text{as} \quad r\to\infty, \quad (13)$$

while θ is exponentially small.

Having determined the forms of the series it is a straightforward matter to generate the governing equations for the coefficient functions and perform asymptotic matching in the usual manner (see (6)); the full details will thus be omitted.

In the results, the eigensolution $(\bar{f}_2, \bar{g}_2)$ has been written in the form

$$(\bar{f}_2, \bar{g}_2)=\lambda(\mathscr{F}, \mathscr{G}), \quad (14)$$

where $\mathscr{F}$, $\mathscr{G}$ are eigenfunctions satisfying the governing equations and boundary conditions, together with the normalizing condition $\mathscr{G}'(0)=1$. The eigenconstant λ is determined by ensuring that (f_2, g_2) satisfy the appropriate boundary conditions: this process is akin to that adopted by Merkin (**12**).

The solution for (f_2, g_2) is non-unique, since arbitrary multiples of $(\mathscr{F}, \mathscr{G})$ are involved.

4. The asymptotic structure as $r\to\infty$ for the inclined case

We now consider the case where $|\delta|<\frac{1}{2}\pi$, that is, the heated surface lies at a finite angle above the horizontal. Proceeding as for the horizontal configuration, the form of the solution valid near the heated boundary is

$$\left.\begin{aligned}\psi&\sim x^{\frac{1}{2}}\bar{f}_0(\zeta)+\bar{f}_1(\zeta)+x^{-\frac{1}{2}}\ln x\,\hat{f}_2(\zeta)+x^{-\frac{1}{2}}\bar{f}_2(\zeta)+\ldots,\\ \theta&\sim\bar{g}_0(\zeta)+x^{-1}\ln x\,\hat{g}_2(\zeta)+x^{-1}\bar{g}_2(\zeta)+\ldots,\end{aligned}\right\} \quad (15)$$

as $x\to\infty$, where

$$\zeta=y/x^{\frac{1}{2}}. \quad (16)$$

The corresponding expansions in the outer region are

$$\left.\begin{aligned}&\psi\sim r^{\frac{1}{2}}\bar{F}_0(\phi)+\bar{F}_2(\phi)+\ldots,\\ &\theta \text{ is exponentially small,}\end{aligned}\right\} \quad \text{as} \quad r\to\infty. \quad (17)$$

Again it is a routine exercise to generate the governing equations and match. For example, the governing system for $(\bar{f}_0, \bar{g}_0)$ is

$$\bar{f}_0''(1+2G\bar{f}_0')=\bar{g}_0'\cos\delta, \quad (18)$$

$$\bar{g}_0''+\tfrac{1}{2}\bar{f}_0\bar{g}_0'=0, \quad (19)$$

with

$$\tilde{g}_0(0)=1, \quad \tilde{f}_0(0)=0, \qquad \tilde{f}_0', \tilde{g}_0 \to 0 \quad \text{as} \quad \zeta\to\infty. \tag{20}$$

By introducing

$$\tilde{f}_0(\zeta)=(\cos\delta)^{\frac{1}{2}}r(t), \qquad \tilde{g}_0(\zeta)=s(t), \qquad \zeta=(\cos\delta)^{-\frac{1}{2}}t, \tag{21}$$

this system simplifies to

$$r''+2Hr'r''=s', \tag{22}$$

$$s''+\tfrac{1}{2}rs'=0, \tag{23}$$

with

$$r(0)=0, \quad s(0)=1, \qquad r', s\to 0 \quad \text{as} \quad t\to\infty, \tag{24}$$

where the one essential parameter H is equal to $G\cos\delta$.

In this inclined case the problem for $(\hat{f}_2, \hat{g}_2)$ possesses leading-edge shift eigensolutions, so that

$$(\hat{f}_2, \hat{g}_2)=\hat{\lambda}(\hat{\mathscr{F}}, \hat{\mathscr{G}}), \tag{25}$$

with

$$\hat{\mathscr{F}}=(\zeta\tilde{f}_0'-\tilde{f}_0)/\tilde{g}_0'(0), \qquad \hat{\mathscr{G}}=[\zeta\tilde{g}_0']/\tilde{g}_0'(0), \tag{26}$$

where the normalizing condition $\hat{\mathscr{G}}'(0)=1$ has been employed. We determine $\hat{\lambda}$ in the same way as λ in the horizontal case.

5. Surface heat transfer

The local surface heat flux q_w into the saturated region is given by

$$q_w=-k_c\left(\frac{\partial T}{\partial y'}\right)_{y'=0}, \tag{27}$$

where k_c is the effective thermal conductivity defined by

$$k_c=(1-\varepsilon)k_m+\varepsilon k_f,$$

with k_m, k_f denoting the thermal conductivities of the matrix material and fluid, respectively, and ε the porosity of the medium. In terms of dimensionless quantities, we have

$$q_w=-\frac{g\beta k[\rho(T_1-T_0)]^2c_p}{\mu}\left(\frac{\partial\theta}{\partial y}\right)_{y=0}, \tag{28}$$

after using $\kappa=k_c/\rho c_p$, where c_p is the specific heat of the fluid. Now from sections 3 and 4, we know the asymptotic forms of $(\partial\theta/\partial y)_{y=0}$ for large x:

$$\frac{\partial\theta}{\partial y}\sim\begin{cases} x^{-\frac{1}{3}}[g_0'(0)+\lambda x^{-\frac{2}{3}}\ln x+O(x^{-\frac{2}{3}})], & \text{(horizontal case)} \quad (29)\\ x^{\frac{1}{2}}[\tilde{g}_0'(0)+\hat{\lambda}x^{-1}\ln x+O(x^{-1})], & \text{(inclined case)} \quad (30)\end{cases}$$

and so we may compute the local heat transfer. We cannot, however, compute the total transfer Q_w from the hot surface between $x=0$

and $x = X$:

$$Q_w = \int_0^X q_w \, dx, \tag{31}$$

because our results are strictly asymptotic. Nevertheless global heat-transfer results can be obtained by calculating the thermal flux at any cross-section of the boundary layer,

$$\begin{aligned} Q_f &= \int_{\substack{\text{boundary} \\ \text{layer}}} \left(\rho c_p u (T - T_0) - k_c \frac{\partial T}{\partial x'} \right) dy' \\ &= \frac{g\beta k [\rho (T_1 - T_0)]^2 c_p}{\mu} \int_0^\infty \frac{\partial \psi}{\partial y} \theta \, dy - k_c (T_1 - T_0) \int_0^\infty \frac{\partial \theta}{\partial x} \, dy. \end{aligned} \tag{32}$$

This quantity Q_f, evaluated at $x = X$ with $X \gg 1$, must be equal (to algebraic orders) to the total surface heat transfer Q_w (defined above) and can be evaluated by using our asymptotic results. Thus,

$$\int_0^\infty \frac{\partial \psi}{\partial y} \theta \, dy \sim \begin{cases} h_0 x^{\frac{1}{3}} + h_1 + h_2 x^{-\frac{1}{3}} \ln x + O(x^{-\frac{1}{3}}) & \text{(horizontal case)} \quad (33) \\ \tilde{h}_0 x^{\frac{1}{2}} + \tilde{h}_1 + \tilde{h}_2 x^{-\frac{1}{2}} \ln x + O(x^{-\frac{1}{2}}) & \text{(inclined case)} \quad (34) \end{cases}$$

where

$$h_0 = \int_0^\infty f_0' g_0 \, d\eta, \qquad h_1 = \int_0^\infty f_1' g_0 \, d\eta, \qquad h_2 = \int_0^\infty (\bar{f}_2' g_0 + f_0' \bar{g}_2) \, d\eta, \tag{35}$$

and

$$\tilde{h}_0 = \int_0^\infty \bar{f}_0' \bar{g}_0 \, d\zeta, \qquad \tilde{h}_1 = \int_0^\infty \bar{f}_1' \bar{g}_0 \, d\zeta, \qquad \tilde{h}_2 = \int_0^\infty (\hat{f}_2' \bar{g}_0 + \bar{f}_0' \hat{g}_2) \, d\zeta. \tag{36}$$

A little manipulation involving the governing differential equations yields that

$$h_0 = -3 g_0'(0), \qquad h_2 = 3\lambda, \tag{37}$$

and

$$\tilde{h}_0 = -2 \bar{g}_0'(0), \qquad \tilde{h}_2 = 2\hat{\lambda}. \tag{38}$$

These four terms in Q_f have their associates in Q_w, but the $(h_1, \tilde{h}_1)$-terms do not—they must therefore be strongly associated with the leading-edge contribution to Q_w. The conduction terms in (32) are of the same order as the remainder terms in (33) and (34) for the horizontal and inclined cases, respectively.

6. Results and discussion

The results of numerically solving the governing differential equations are shown in Figs 2 to 14 and Tables 1 to 4. They were obtained by using a

Runge–Kutta–Merson procedure with either a shooting method or the method of complementary functions, as appropriate. Using these results, the physical velocity components

$$(u, v) = \left[\frac{g\beta(T_1 - T_0)k\rho}{\mu}\right]\left(\frac{\partial\psi}{\partial y}, -\frac{\partial\psi}{\partial x}\right)$$

and temperature

$$T = T_0 + (T_1 - T_0)\theta$$

may be calculated, together with the heat-transfer data described in section 5.

For the horizontal configuration we have

$$\begin{aligned} \partial\psi/\partial y &= x^{-\frac{1}{3}}f_0'(\eta) + x^{-\frac{2}{3}}f_1'(\eta) + \lambda x^{-1}\ln x\,\mathscr{F}'(\eta) + O(x^{-1}), \\ -\partial\psi/\partial x &= x^{-\frac{2}{3}}[\tfrac{2}{3}\eta f_0'(\eta) - \tfrac{1}{3}f_0(\eta)] + \tfrac{2}{3}x^{-1}\eta f_1'(\eta) + \\ &\quad + \lambda x^{-\frac{4}{3}}\ln x\,[\tfrac{2}{3}\eta\mathscr{F}'(\eta) + \tfrac{1}{3}\mathscr{F}(\eta)] + O(x^{-\frac{4}{3}}), \end{aligned}$$

and

$$\theta = g_0(\eta) + \lambda x^{-\frac{2}{3}}\ln x\,\mathscr{G}(\eta) + O(x^{-\frac{2}{3}}).$$

The results pertaining to this case are shown in Figs 2 to 4 and Tables 1, 2.

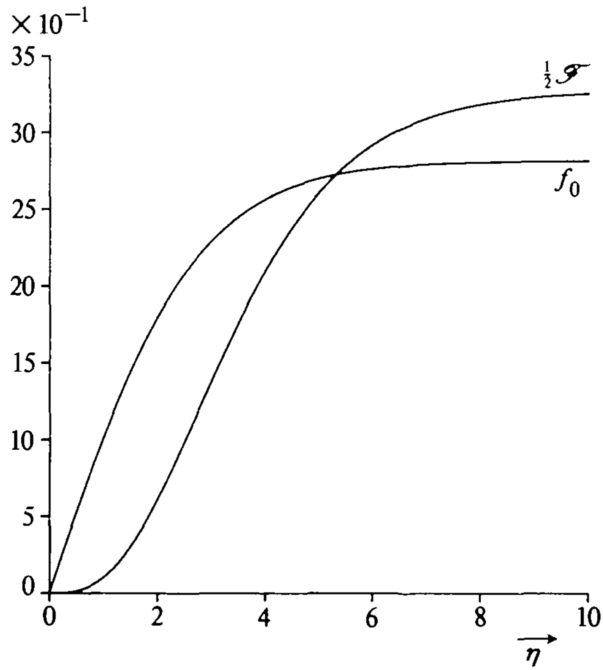

FIG. 2. Horizontal boundary-layer functions f_0, $\frac{1}{2}\mathscr{F}$

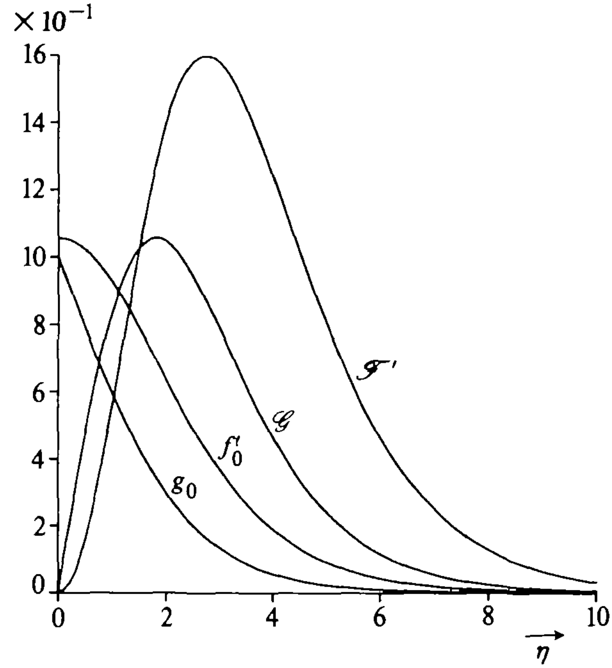

FIG. 3. Horizontal boundary-layer functions f_0', $\mathscr{F}'$, g_0, $\mathscr{G}$

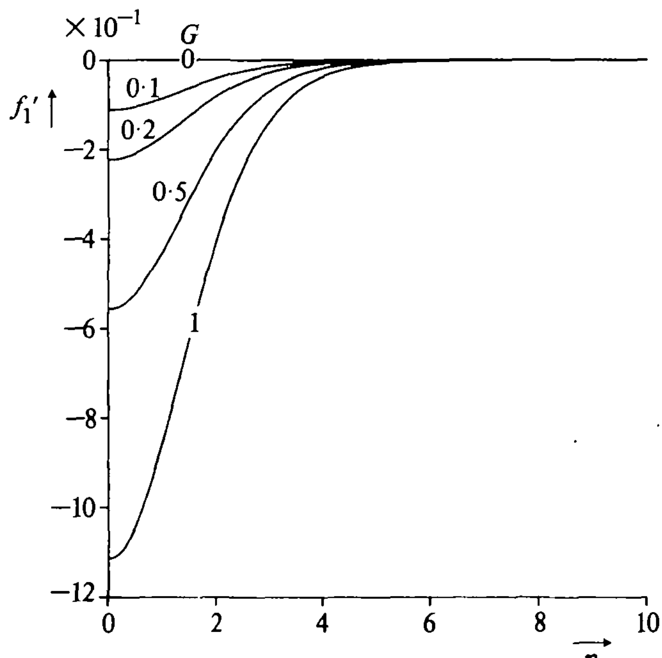

FIG. 4. Behaviour of the horizontal boundary-layer function f_1' for $G = 0$, 0·1, 0·2, 0·5 and 1. The wedge angle in the illustration is $\frac{3}{2}\pi$; results for other wedge angles may be obtained by a shift in the vertical axis according to equation (39)

TABLE 1. *Variation of λ with α and G in the horizontal configuration*

	λ					
α	$G=0$	$G=0{\cdot}01$	$G=0{\cdot}1$	$G=1$	$G=10$	$G=100$
$\frac{1}{2}\pi$	0	0·014	0·146	0·301	0·821	1·870
π	0	0·005	0·060	0·128	0·390	1·008
$\frac{3}{2}\pi$	0	0·002	0·021	0·050	0·194	0·616

TABLE 2. *Variation of the convective heat-transfer coefficient h_1 with α and G in the horizontal configuration*

	h_1					
α	$G=0$	$G=0{\cdot}01$	$G=0{\cdot}1$	$G=1$	$G=10$	$G=100$
$\frac{1}{2}\pi$	−2·575	−2·586	−2·691	−2·807	−3·157	−3·739
π	−0·858	−0·870	−0·975	−1·091	−1·440	−2·023
$\frac{3}{2}\pi$	0	−0·012	−0·116	−0·233	−0·582	−1·164

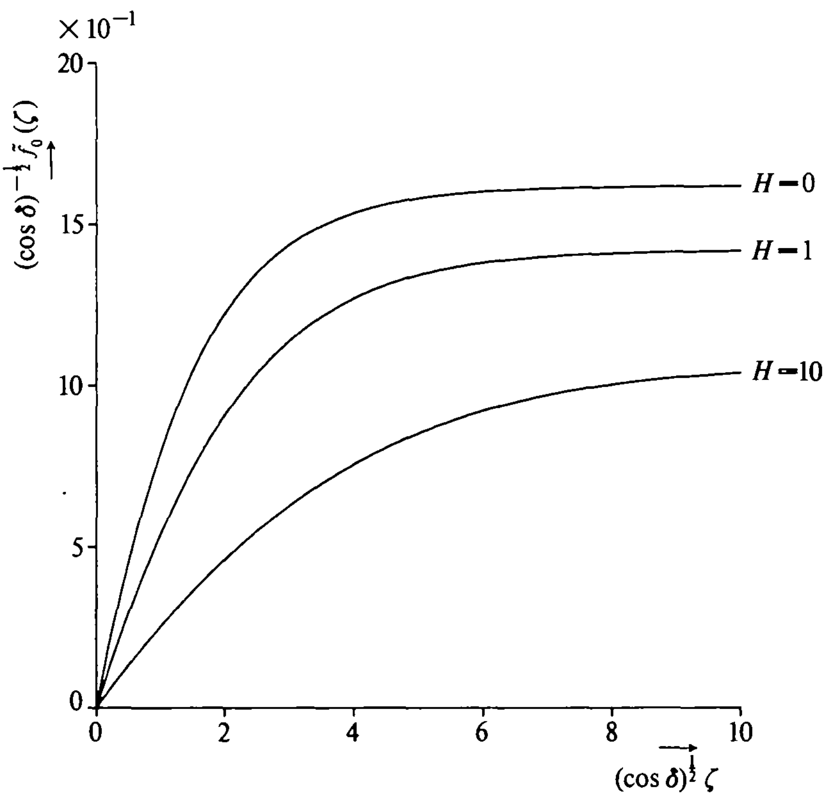

FIG. 5. Boundary-layer function $\tilde{f}_0$

The stream functions f_0 and $\mathscr{F}$ are displayed in Fig. 2, whilst the corresponding effective horizontal velocity and thermal profiles are in Fig. 3. Note that both the zeroth- and second-order functions are independent of the wedge angle α and parameter G. Figure 4 shows the effect of varying G, for fixed α, on the first-order velocity f_1'. This velocity is zero in the Darcy case and, as the departure from the Darcian regime increases (that is, as G increases), this velocity becomes more negative, implying that as the inertial effects grow the induced velocity decreases. The effect of varying the wedge angle on f_1' is given by the simple shift

$$f_1' = -Gf_0'^2 - \tfrac{1}{3}a_0 \cot(\tfrac{1}{3}\alpha), \tag{39}$$

so that f_1' increases as α increases. Table 1, which gives the values of λ for various α and G, together with the fact that

$$g_0'(0) = -0{\cdot}4302,$$

enables the local heat transfer to be calculated from (28) and (29). Table 2

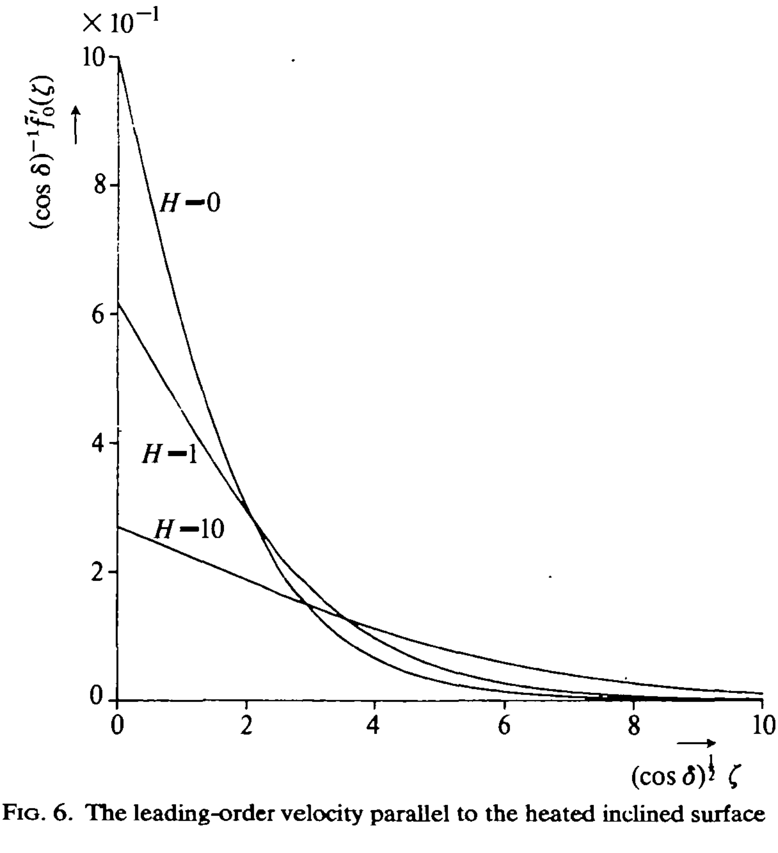

FIG. 6. The leading-order velocity parallel to the heated inclined surface

gives the convective heat-transfer coefficient h_1 which facilitates the computation of the global heat transfer from (32), (33) and (34). Clearly the heat transfer falls as G increases or as the wedge angle decreases, which is consistent with the velocity behaviour, as this also decreases. Finally it is noted that as $G \to 0$, $\lambda \to 0$ which is consistent with the analysis in (**5**) of the Darcy case.

For the inclined configuration

$$\begin{aligned} \partial\psi/\partial y &= \tilde{f}_0'(\zeta) + x^{-\frac{1}{2}}\tilde{f}_1'(\zeta) + \hat{\lambda}x^{-1}\ln x\,\hat{\mathscr{F}}'(\zeta) + O(x^{-1}), \\ -\partial\psi/\partial x &= x^{-\frac{1}{2}}[\tfrac{1}{2}\zeta\tilde{f}_0'(\zeta) - \tfrac{1}{2}\tilde{f}_0(\zeta)] + \tfrac{1}{2}x^{-1}\zeta\tilde{f}_1'(\zeta) + \\ &\quad + \hat{\lambda}x^{-\frac{3}{2}}\ln x[\tfrac{1}{2}\zeta\hat{\mathscr{F}}'(\zeta) + \tfrac{1}{2}\hat{\mathscr{F}}(\zeta)] + O(x^{-\frac{3}{2}}), \end{aligned}$$

and

$$\theta = \tilde{g}_0(\zeta) + \hat{\lambda}x^{-1}\ln x\,\hat{\mathscr{G}}(\zeta) + O(x^{-1}).$$

The results for this inclined case, which are presented in Figs 5 to 14 and Tables 3 and 4, are more involved than the horizontal case because of the

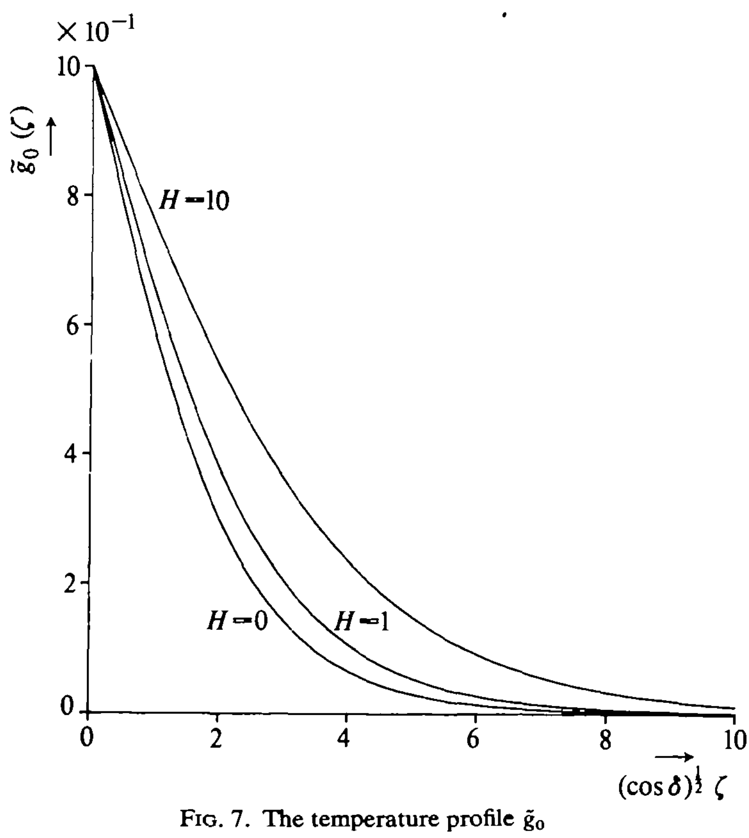

FIG. 7. The temperature profile $\tilde{g}_0$

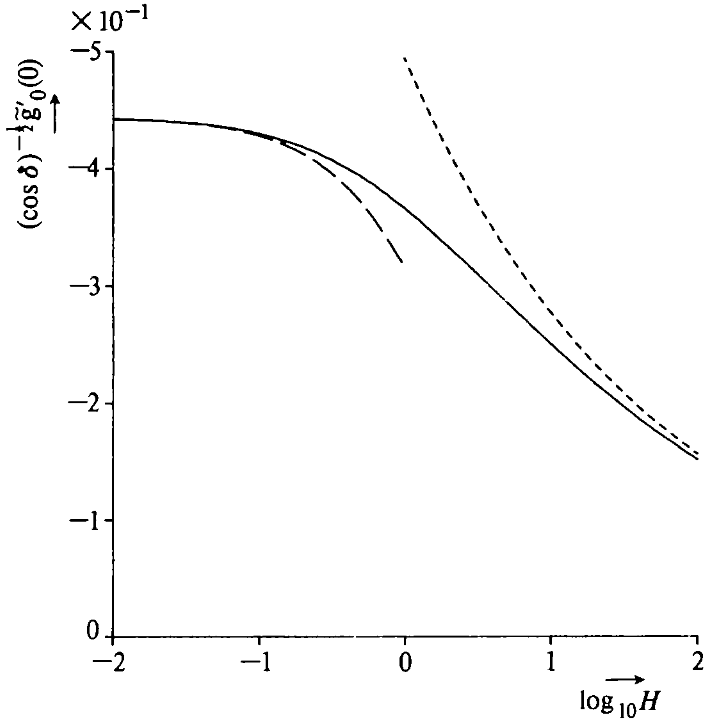

FIG. 8. Variation of the dimensionless heat transfer $-g_0'(0)$ with H: —— asymptotic results for $H \ll 1$; - - asymptotic results for $H \gg 1$

dependency on the parameter G and on the angle that the heated surface makes with the gravity vector δ. Three different attitudes of the heated surface have been considered—vertical, that is parallel to the gravity vector, and at $\frac{1}{4}\pi$ to the vertical facing upwards and downwards, respectively. In conjunction with this, the effect of wedge angle has been examined: angles of $\frac{1}{4}\pi$, $\frac{1}{2}\pi$, π and $\frac{3}{2}\pi$ were taken.

Figures 5, 6 and 7 display, for various H, the zeroth-order stream function, the velocity parallel to the heated surface, and thermal profiles. The variation of the zeroth-order wall heat transfer with H is shown in Fig. 8, together with the asymptotic results

$$\tilde{g}_0'(0) \sim \begin{cases} -0{\cdot}4438 + 0{\cdot}1636 * H - 0{\cdot}03538 * H^2 & \text{for } H \ll 1, \\ -0{\cdot}4938 * H^{-\frac{1}{3}} & \text{for } H \gg 1, \end{cases}$$

which follow from (22) to (24). The first-order 'velocities' $\tilde{f}_1'$ are plotted in Figs 9, 10 and 11 for the three heated-plate attitudes, respectively. These velocities increase as the heated plate is rotated clockwise or as the wedge angle increases or as G increases. Moreover it may be shown that $\tilde{f}_1'(\delta, \alpha) = -\tilde{f}_1'(-\delta, 2\pi - \alpha)$ as confirmed by the graphs. Figures 12 to 14 are the

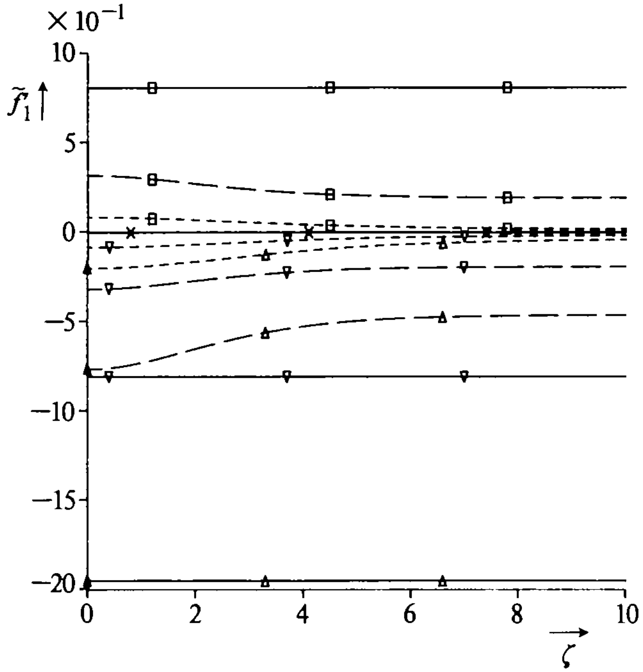

FIG. 9. Behaviour of the first-order boundary-layer function $\bar{f}_1'$ when $\delta = 0$: ———— $G = 0$; — — — — $G = 1$; ------ $G = 10$. □: $\alpha = \frac{3}{2}\pi$; ×: $\alpha = \pi$; ∇: $\alpha = \frac{1}{2}\pi$; △: $\alpha = \frac{1}{4}\pi$. The graphs for $\alpha = \pi$, $G = 0$, 1 and 10 are all coincident

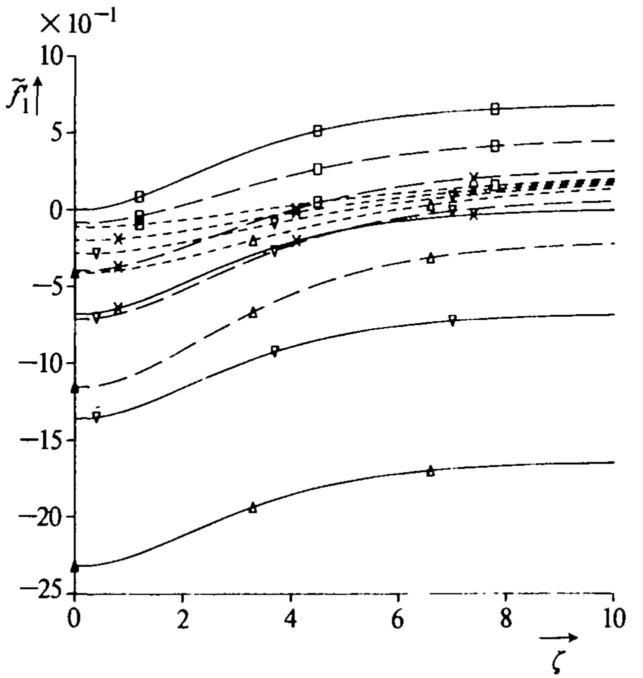

FIG. 10. Behaviour of the first-order boundary-layer function $\bar{f}_1'$ when $\delta = \frac{1}{4}\pi$: ———— $G = 0$; — — — — $G = 1$; ------ $G = 10$. □: $\alpha = \frac{3}{2}\pi$; ×: $\alpha = \pi$; ∇: $\alpha = \frac{1}{2}\pi$; △: $\alpha = \frac{1}{4}\pi$

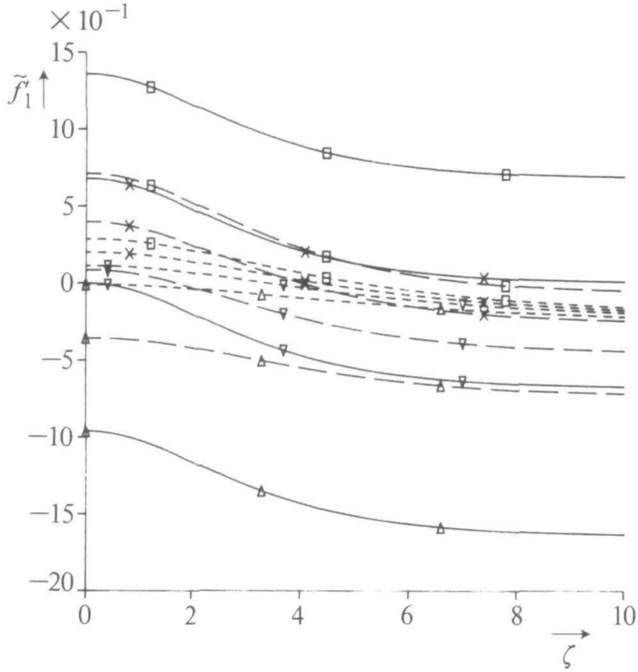

FIG. 11. Behaviour of the first-order boundary-layer function f_1' when $\delta = \frac{1}{4}\pi$: ———— $G = 0$; — — — $G = 1$; - - - - - $G = 10$. $\square$: $\alpha = \frac{3}{2}\pi$; $\times$: $\alpha = \pi$; ∇: $\alpha = \frac{1}{2}\pi$; $\triangle$: $\alpha = \frac{1}{4}\pi$

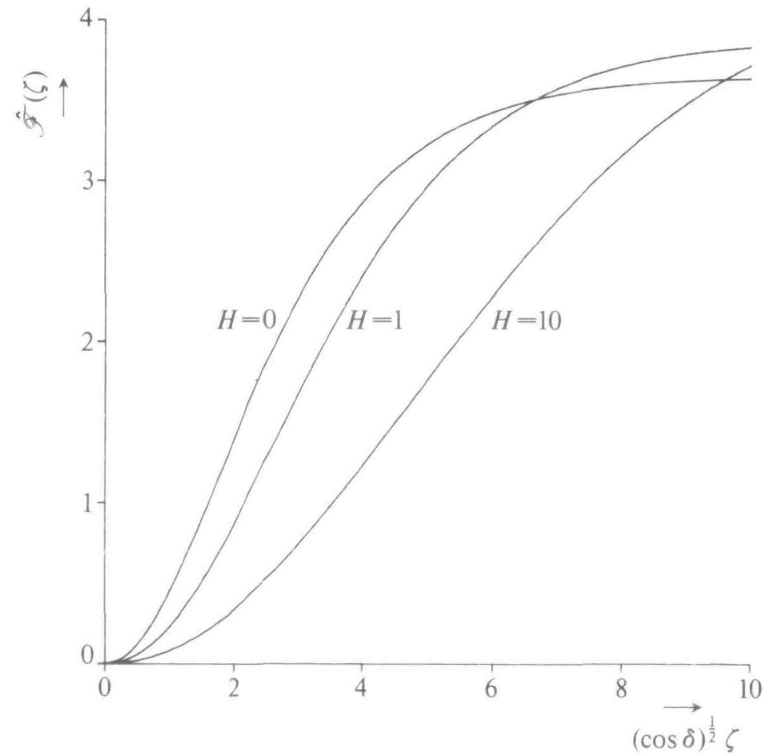

FIG. 12. Comparison of $\hat{\mathscr{F}}$ for $H = 0$, 1 and 10

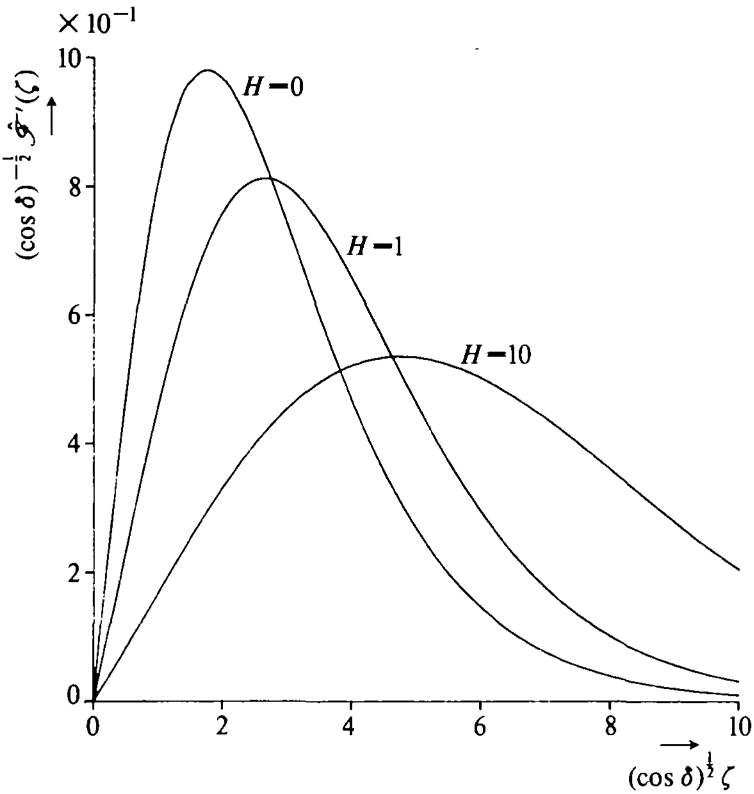

FIG. 13. Comparison of $\hat{\mathcal{F}}'$ for $H=0$, 1 and 10

second-order analogues of Figs 5 to 7 (the solutions are symmetric with respect to δ).

The local heat transfer may be calculated from (28) and (30) using Fig. 8 to obtain $\tilde{g}_0'(0)$ and Table 3 for $\hat{\lambda}$. Furthermore, the global heat transfer may be obtained from (32), (33) and (38) if reference is also made to Table 4, which gives the coefficient $\bar{h}_1$. The general trend is that the heat transfer decreases if (i) the heated surface is inclined away from the vertical, (ii) the wedge angle is decreased, or (iii) G is increased. It is interesting to note that the behaviour of $\hat{\lambda}$ with G is not monotonic (see Table 4). Again in the vertical case we note that $\hat{\lambda} \to 0$ as $G \to 0$ consistent with the analysis of the Darcy case presented in (6). For the inclined cases, however, $\hat{\lambda} \not\to 0$ as $G \to 0$, so that the logarithms remain, even for Darcy flow. Thus the mechanism described in (6) for the generation of logarithmic terms, although still present in the inclined case, is of prime importance only in the vertical case.

Finally, the analysis presented in this paper may be easily extended to cover cooled surfaces at inclinations $|\delta| > \frac{1}{2}\pi$ and downward-facing horizontal cooled surfaces. It may also be extended for non-isothermal horizontal

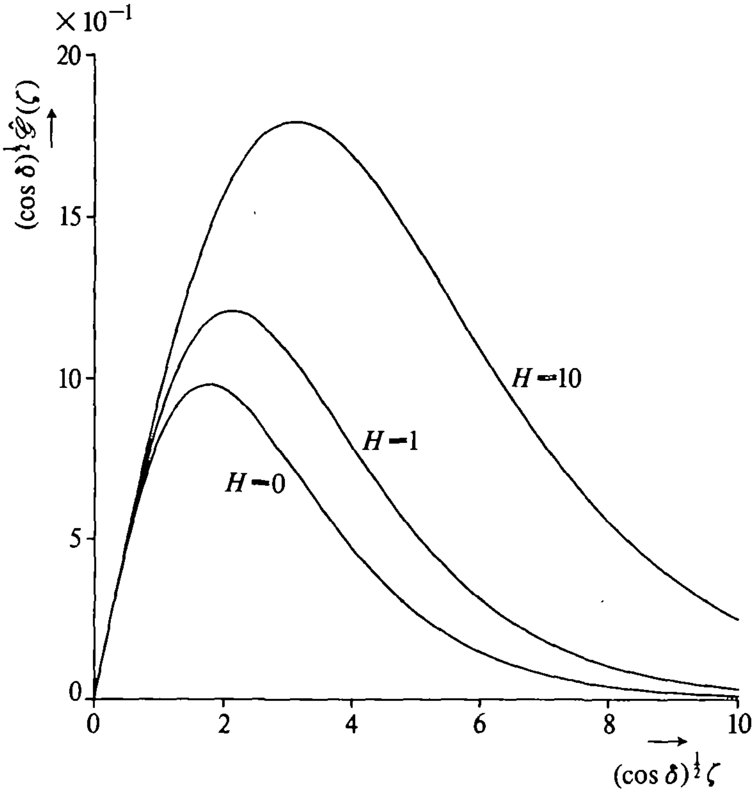

FIG. 14. Comparison of the second-order thermal profiles $\hat{\mathscr{G}}$ for $H=0$, 1 and 10

TABLE 3. *Variation of $\hat{\lambda}$ with α, δ and G*

		$\hat{\lambda}$			
α	δ	$G=0$	$G=0\cdot1$	$G=1$	$G=10$
$\frac{1}{4}\pi$	0	0	0·146	0·286	0·126
$\frac{1}{2}\pi$	0	0	0·030	0·055	−0·001
π	0	0	−0·008	−0·048	−0·170
$\frac{3}{2}\pi$	0	0	−0·056	−0·309	−0·965
$\frac{1}{4}\pi$	$-\frac{1}{4}\pi$	1·536	1·606	1·509	0·923
$\frac{1}{2}\pi$	$-\frac{1}{4}\pi$	0·768	0·756	0·654	0·429
π	$-\frac{1}{4}\pi$	0·384	0·364	0·287	0·098
$\frac{3}{2}\pi$	$-\frac{1}{4}\pi$	0·256	0·222	0·006	−0·739
$\frac{1}{4}\pi$	$\frac{1}{4}\pi$	−1·536	−1·303	−0·727	−0·375
$\frac{1}{2}\pi$	$\frac{1}{4}\pi$	−0·768	−0·711	−0·500	−0·237
π	$\frac{1}{4}\pi$	−0·384	−0·398	−0·378	−0·277
$\frac{3}{2}\pi$	$\frac{1}{4}\pi$	−0.256	−0·344	−0·612	−1·071

TABLE 4. *Variation of the convective heat-transfer coefficient* $\tilde{h}_1$ *with* α, δ *and* G

α	δ	$\tilde{h}_1$ $G=0$	$G=0{\cdot}1$	$G=1$	$G=10$
$\frac{1}{4}\pi$	0	$-3{\cdot}153$	$-2{\cdot}623$	$-1{\cdot}310$	$-0{\cdot}423$
$\frac{1}{2}\pi$	0	$-1{\cdot}306$	$-1{\cdot}087$	$-0{\cdot}543$	$-0{\cdot}175$
π	0	0	0	0	0
$\frac{3}{2}\pi$	0	$1{\cdot}306$	$1{\cdot}087$	$0{\cdot}543$	$0{\cdot}175$
$\frac{1}{4}\pi$	$-\frac{1}{4}\pi$	$-4{\cdot}153$	$-3{\cdot}627$	$-2{\cdot}037$	$-0{\cdot}500$
$\frac{1}{2}\pi$	$-\frac{1}{4}\pi$	$-2{\cdot}306$	$-2{\cdot}020$	$-1{\cdot}165$	$-0{\cdot}154$
π	$-\frac{1}{4}\pi$	$-1{\cdot}000$	$-0{\cdot}884$	$-0{\cdot}548$	$-0{\cdot}311$
$\frac{3}{2}\pi$	$-\frac{1}{4}\pi$	$0{\cdot}306$	$0{\cdot}252$	$0{\cdot}069$	$-0{\cdot}109$
$\frac{1}{4}\pi$	$\frac{1}{4}\pi$	$-2{\cdot}153$	$-1{\cdot}859$	$-0{\cdot}941$	$-0{\cdot}177$
$\frac{1}{2}\pi$	$\frac{1}{4}\pi$	$-0{\cdot}306$	$-0{\cdot}252$	$-0{\cdot}069$	$0{\cdot}109$
π	$\frac{1}{4}\pi$	1	$0{\cdot}884$	$0{\cdot}548$	$0{\cdot}311$
$\frac{3}{2}\pi$	$\frac{1}{4}\pi$	$2{\cdot}306$	$2{\cdot}020$	$1{\cdot}165$	$0{\cdot}514$

surfaces with power-law temperature variations, but, when $G \neq 0$, the inclined-surface case apparently does not admit similarity solutions to the zeroth-order problem for such general variations.

Acknowledgement

The second author would like to thank the SERC for the Research Studentship which enabled this research to be undertaken.

REFERENCES

1. J. BEAR, *Dynamics of Fluids in Porous Media* (Elsevier, New York, 1972).
2. P. CHENG and I-DEE CHANG, *Int. J. Heat Mass Transfer* **19** (1976) 1267–1272.
3. —— and W. J. MINKOWYCZ, *J. Geophys. Res.* **82** (1977) 2040–2044.
4. C. H. JOHNSON and P. CHENG, *Int. J. Heat Mass Transfer* **21** (1978) 669–676.
5. I-DEE CHANG and P. CHENG, *ibid.* **26** (1983) 163–174.
6. P. G. DANIELS and P. G. SIMPKINS, *Q. Jl Mech. appl. Math.* **37** (1984) 339–354.
7. O. A. PLUMB and J. C. HUENEFELD, *Int. J. Heat Mass Transfer* **24** (1981) 765–768.
8. D. R. JONES, *Q. Jl Mech. appl. Math.* **26** (1973) 77–98.
9. D. A. S. REES and D. S. RILEY, *Int. J. Heat Mass Transfer*, to appear.
10. K. STEWARTSON, *J. Math. Phys.* **36** (1957) 173–191.
11. C. A. HEIBER, *Int. J. Heat Mass Transfer* **17** (1974) 785–791.
12. J. H. MERKIN, *J. Fluid Mech.* **35** (1969) 439–450.
13. A. BEJAN and D. POULIKAKOS, *ibid.* **27** (1984) 717–722.